Influences on neural lineage and mode of division in the zebrafish retina in vivo

Lucia Poggi,[1] Marta Vitorino,[1] Ichiro Masai,[2] and William A. Harris[1]

[1]Department of Anatomy, University of Cambridge, Cambridge CB2 3DY, United Kingdom
[2]RIKEN Institute of Physical and Chemical Research, Hirosawa, Saitama 351-0198, Japan

Cell determination in the retina has been under intense investigation since the discovery that retinal progenitors generate clones of apparently random composition (Price, J., D. Turner, and C. Cepko. 1987. *Proc. Natl. Acad. Sci. USA*. 84:156–160; Holt, C.E., T.W. Bertsch, H.M. Ellis, and W.A. Harris. 1988. *Neuron*. 1:15–26; Wetts, R., and S.E. Fraser. 1988. *Science*. 239:1142–1145). Examination of fixed tissue, however, sheds little light on lineage patterns or on the relationship between the orientation of division and cell fate. In this study, three-dimensional time-lapse analyses were used to trace lineages of retinal progenitors expressing green fluorescent protein under the control of the *ath5* promoter. Surprisingly, these cells divide just once along the circumferential axis to produce two postmitotic daughters, one of which becomes a retinal ganglion cell (RGC). Interestingly, when these same progenitors are transplanted into a mutant environment lacking RGCs, they often divide along the central-peripheral axis and produce two RGCs. This study provides the first insight into reproducible lineage patterns of retinal progenitors in vivo and the first evidence that environmental signals influence the orientation of cell division and the lineage of neural progenitors.

Introduction

Isolated retinal progenitors give rise to clones of cells in vitro that are similar in size and cellular composition to clones that such progenitors generate in vivo (Cayouette et al., 2003). This suggests the existence of preestablished lineage programs in retinal progenitors. But what are these programs and what factors control them?

The ath5, a bHLH transcription factor, is necessary and sufficient for the development of retinal ganglion cells (RGCs), which are the earliest born cell type in the vertebrate retina (Kanekar et al., 1997; Brown et al., 2001; Kay et al., 2001; Wang et al., 2001). In *ath5* mutants, there is a delay in the first cells to exit the cell cycle, which is consistent with the failure of any population of cells to exit the cell cycle at the time when RGCs are normally born. Similarly, when ath5 is transfected into retinal progenitors, those cells tend to leave the cell cycle early in histogenesis at the time when RGCs are normally born, and then about half of these cells become RGCs (Ohnuma et al., 2002). In a recent study, an ath5:GFP transgenic line faithfully recapitulating *ath5* expression in the zebrafish retina was used to show that ath5 and RGC determination is switched on in a spatio-temporal pattern that depends on intrinsic properties of the neuroblasts themselves (Kay et al., 2005). Together, these data are consistent with the idea that the lineage of neuroblasts is determined by the expression of ath5.

Although recent findings suggest that cell-intrinsic properties of neuroblasts play a major role in affecting the cell lineage during retinal development (Cayouette et al., 2003; Kay et al., 2005; Mu et al., 2005), environmental factors have also been proposed to affect the lineage of retinal progenitors. In particular, negative feedback from developing RGCs has been shown to limit the production of new RGCs (Waid and McLoon, 1998; Gonzalez-Hoyuela et al., 2001). This is known because ganglion cell production can be restored in these progenitors when ganglion cells are depleted from the older cell population. Interestingly, selective depletion of RGCs in the differentiating mouse retina in vivo leads to an increase in the number of progenitors expressing *ath5* (Mu et al., 2005), providing a possible link between extrinsic and intrinsic coordination of cell division and cell fate.

For these reasons, we wanted to see whether ath5-expressing progenitors showed any reproducible lineage patterns and whether these patterns could be influenced by negative feedback. We reasoned that the best way to see these things was by using an in vivo time-lapse approach.

Correspondence to William A. Harris: harris@mole.bio.cam.ac.uk

Abbreviations used in this paper: 3D, three dimensional; GAP, growth-associated protein; GCL, ganglion cell layer; INL, inner nuclear layer; ONL, outer nuclear layer; RGC, retinal ganglion cell.

The online version of this article contains supplemental material.

The Journal of Cell Biology, Vol. 171, No. 6, December 19, 2005 991–999
http://www.jcb.org/cgi/doi/10.1083/jcb.200509098

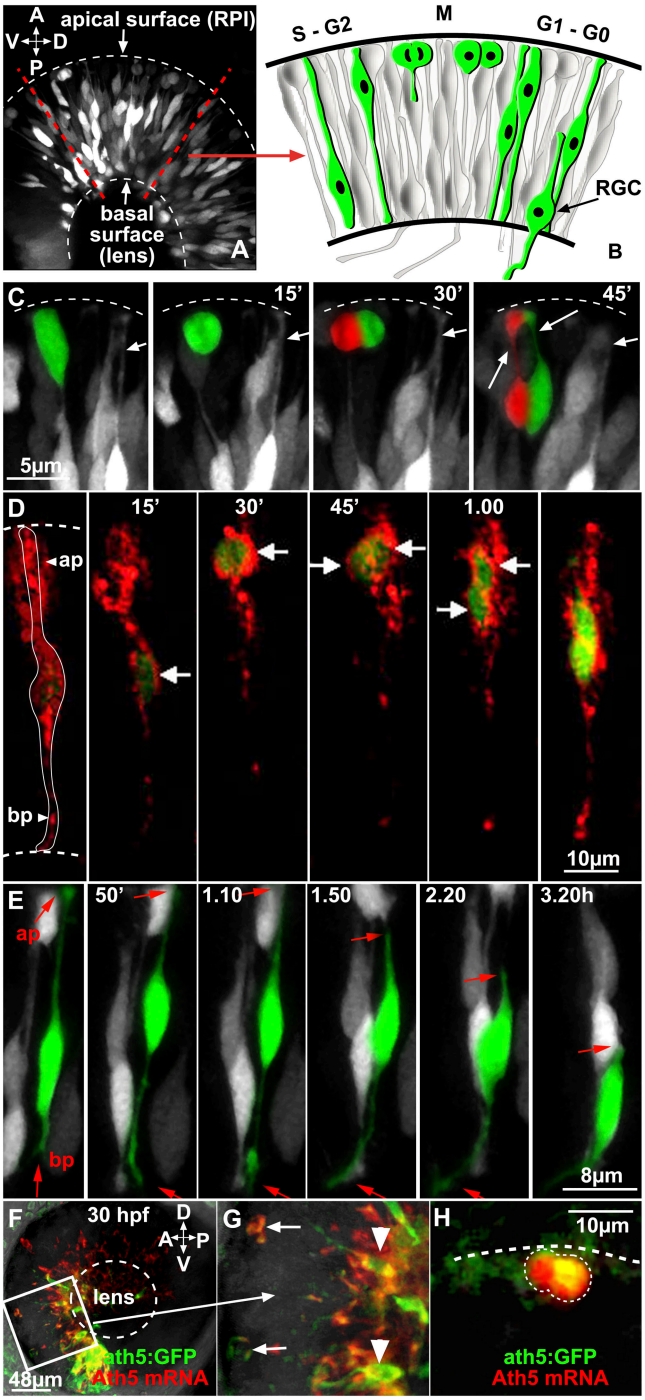

Figure 1. **ath5:GFP is expressed in both mitotic and differentiating retinal progenitors.** (A) 3D lateral view of an ath5:GFP transgenic retina at 32 h after fertilization, as seen in all subsequent time-lapse recordings performed in this study (the image is a combination of several stacks). The diagram in B shows the main developmental steps of one retinal neuroepithelial cell. The cell soma undergoes apico-basal interkinetic nuclear movements. Mitosis (M) occurs in proximity of the apical surface (top). (C) Time-lapse series showing an ath5:GFP progenitor dividing at the apical surface (dashed line). Dividing progenitors and daughter cells are highlighted in green or red. The long arrows point at the apical processes that connect the ath5:GFP retinal progenitors to the apical surface. Short arrows point to the apical process of a differentiating ath5-positive cell. This process can be seen retracting in the right-most panel. (D) A single retinal progenitor cell is labeled with GAP-mRFP. The time-lapse series shows that ath5:GFP appears ($t = 0$) when the cell soma is migrating toward the apical surface (ap). At $t = 45$ min, the cell divides and both daughter cells migrate basally. White arrows indicate the position of the cell soma of the progenitor or daughter cells. (E) Time-lapse sequence showing the sequential steps of RGC differentiation (also see the diagram in B). The cell highlighted in green is expressing ath5:GFP. At $t = 0$, the cell is connected to the apical and basal surface with its apical and basal processes, respectively. Later on, the apical process (ap and arrows) retracts from the apical surface ($t = 1.50$), and the axon starts to elongate and extend from the basal process (bp and arrows). (F–H) Confocal images of an ath5:GFP transgenic retina at 30 h after fertilization, hybridized with *ath5* mRNA probe (in red). Each image is a projection of stacks. The white box indicates what is represented in G. Arrows point at two dividing progenitors at the apical surface that are expressing both ath5:GFP and *ath5* mRNA, although clearly at different amounts. Arrowheads point at differentiating RGCs. (H) 3D representation of a dividing ath5:GFP cell (outlined) expressing *ath5* mRNA. A, anterior; ap; apical process; bp, basal process; D, dorsal; P, posterior; RGC, retinal ganglion cell; RPI, retinal pigmented epithelium; V, ventral.

Time-lapse imaging studies on explanted pieces of developing ferret cortex suggested that the orientation of cell division is associated with different daughter cell fates (Chenn and McConnell, 1995). Similarly, the examination of rat retinal explants revealed that daughters with similar fates derived mostly from divisions in the plane of the retinal surface, whereas orthogonal (apical-basal) divisions generated different daughter cells (Cayouette and Raff, 2003). To reconstruct cell divisions in the fully intact developing retina, researchers turned to the transparent embryonic zebrafish embryo (Das et al., 2003). Three dimensional (3D) time-lapse observations of fluorescently labeled progenitors in this preparation showed that the orientation of cell division shifts from central-peripheral to circumferential over development. Interestingly, that study also showed that the normal shift in the orientation of cell division was affected in the *ath5* mutant *lakritz*, raising the issue of how the orientation of cell division correlates with specific cell fates.

In this study, we used the ath5:GFP transgenic line of zebrafish (Masai et al., 2003) combined with 3D time-lapse video microscopy. This allowed us, for the first time, to determine reproducible features in lineages of *ath5*-expressing progenitors in a normal embryo and to demonstrate that environmental signals affect lineage pattern and orientation of cell division.

Results

ath5-expressing cells go through mitosis before they differentiate

Recent BrdU experiments describe *ath5* expression as a post–S-phase marker of retinal progenitors (Masai et al., 2005). However, GFP driven by the *ath5* promoter and enhancer is detectable before RGCs complete their differentiation and possibly before their final mitosis (Masai et al., 2005). Therefore, we used these transgenic ath5:GFP fish embryos to perform long-term time-lapse imaging of ath5:GFP-expressing retinal progenitors to see when in the cell cycle these cells began to express GFP. Embryonic retinas that were imaged in 15-min intervals with optical sections 0.5 μm apart were taken through a volume up to 50 μm in depth for a minimum of 10 h starting from ~32 h after fertilization (Fig. 1 A). A schematic describing the main features of the developing retinal neuroepithelium

is shown in Fig. 1 B. These image sets were reconstructed into 3D time-lapse videos. ath5:GFP cells could be clearly seen undergoing M phase of the cell cycle at the apical surface (Fig. 1 C and Video 1, available at http://www.jcb.org/cgi/content/full/jcb.200509098/DC1). In a few instances, we transplanted ath5:GFP blastomeres that had been injected with a membrane-targeted RFP construct (growth-associated protein [GAP]–mRFP) and used double labeling to highlight cells as they first turned on GFP. Although the RFP label was weak and faded rather quickly in these experiments, we were able to focus on dividing cells that became GFP positive during the recording sessions. In these cases, GFP first became visible in RFP-labeled cells as the nuclei of these cells were migrating toward the apical surface before metaphase (Fig. 1 D and Video 2). This apically oriented phase of interkinetic nuclear migration is generally associated with the G2 phase of the cell cycle (Seymour and Berry, 1975). Finally, ath5:GFP cells could be seen acquiring the anatomical characteristics of RGCs. Differentiation into RGCs is characterized by the retraction of the apical process, the migration of the cell body to the RGC layer of the retina near the vitreal surface, and the extension of a growth cone–tipped axon that grows along the vitreal surface toward the future optic nerve head (Fig. 1 E and Video 3).

To test the fidelity of GFP expression in these transgenic embryos, we examined *ath5* RNA expression in the retina at stages when these signals first become visible. The level of *ath5* mRNA is unaffected by the expression of GFP from the transgenic promoter, as quantitative RT-PCR analysis reveals that transgenic and wild-type embryos express indistinguishable amounts of *ath5* mRNA (not depicted). Moreover, GFP and *ath5* mRNA can often be seen in the same cells, including dividing precursors (Fig. 1, F–H). These colocalization results agree with and extend those of previous studies (Kay et al., 2005; Masai et al., 2005).

ath5-expressing progenitors divide once and produce one RGC daughter

ath5 is necessary for RGC development, yet not all *ath5*-positive cells differentiate as RGCs. *ath5* mutants of zebrafish (called *lakritz*; Kay et al., 2001) and *Math5* knockouts in mice (Brown et al., 2001; Wang et al., 2001) have a strong reduction in RGCs, whereas lipofection experiments in *Xenopus laevis* show that *Xath5* promotes RGC fate in approximately half of the misexpressing cells (Kanekar et al., 1997). Moreover, the effects of *Xath5* on cell fate appear to be stage dependent; misexpression at early stages primarily promotes RGC fates, whereas the same experiment at later stages promotes other retinal neuronal fates (Moore et al., 2002). *Math5* expression was also found to be associated with the differentiation of multiple retinal neuron types in the developing mouse (Yang et al., 2003) and in developing transgenic *Xenopus* retinas (Hutcheson et al., 2005). These results raise the issue of how *ath5* expression affects the lineage and fate of precursors in vivo during normal development.

ath5 mRNA is rapidly lost from differentiating progenitors and is not visible even in mature RGCs. However, the persistence of stable GFP protein in transgenic zebrafish allowed

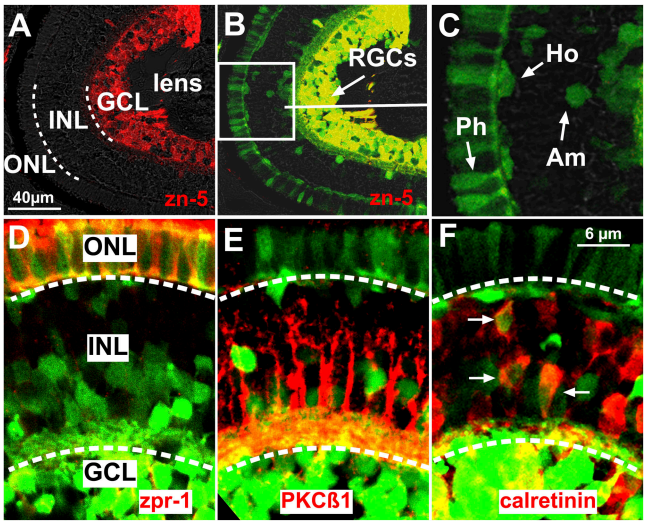

Figure 2. **ath5:GFP cells become RGCs and other cell types in the zebrafish retina.** (A–C) Sections through the central retina of a 5-d ath5:GFP transgenic embryo. (A) The three retinal cell layers are separated by a white dashed line. (B) Retinal ganglion cell (RGC) ath5:GFP progenitors in the ganglion cell layer (GCL) are zn-5+. The white box in B indicates the area shown in C. Some ath5:GFP progenitors (C) become photoreceptors (Ph), amacrines (Am), and horizontal (Ho) cells. (D–F) Sections of 4-d ath5:GFP transgenic embryos immunostained with zpr-1 (D), PKCβ1 (E), and calretinin (F; arrows). White dashed lines separate the three retinal cell layers. ath5:GFP cells colabel with zpr-1 in the outer nuclear layer (ONL) and with calretinin in the inner nuclear layer (INL). ath5:GFP cells in the INL do not colabel with PKCβ1.

us to track the fate of ath5:GFP-positive cells to later stages. Therefore, we analyzed the distribution of positive cells in 5-d postfertilization retinas, when all retinal cell layers are differentiated and distinguishable. Histological sections through the central retina showed GFP-positive cells in the ganglion cell layer (GCL) as expected. These cells colabeled with the RGC-specific antibody zn-5. There were also many GFP-positive cells in the inner nuclear layer (INL) and outer nuclear layer (ONL; Fig. 2, A–C). GFP-positive INL cells could often be identified by their morphologies and positions as either horizontal or amacrine cells (Fig. 2 C). Interestingly, we found that the INL GFP-positive cells do not colabel with the bipolar marker PKCβ1; on the other hand, some colabel with the amacrine-specific marker calretinin (Fig. 2, E and F), further suggesting that at least a number of these INL cells are amacrines. The GFP-positive cells in the ONL had the morphology of photoreceptors and expressed the photoreceptor-specific marker zpr-1 (Fig. 2 D). These results show that RGCs are not the exclusive fate choice of *ath5*-expressing retinal progenitors in the zebrafish retina.

To map out the lineage relationships between the ath5:GFP-positive RGCs and the other ath5:GFP-positive cells in the retina, we examined the dividing ath5:GFP progenitors and followed their descendents by 3D time lapse. This was difficult to do in the "normal" transgenic fish embryos because the high density of ath5:GFP-positive cells made it difficult to pick out lineages in our time-lapse videos. Therefore, to see these progenitors more clearly, we transplanted blastula-stage cells from ath5:GFP transgenic fish into the blastulas of nontransgenic

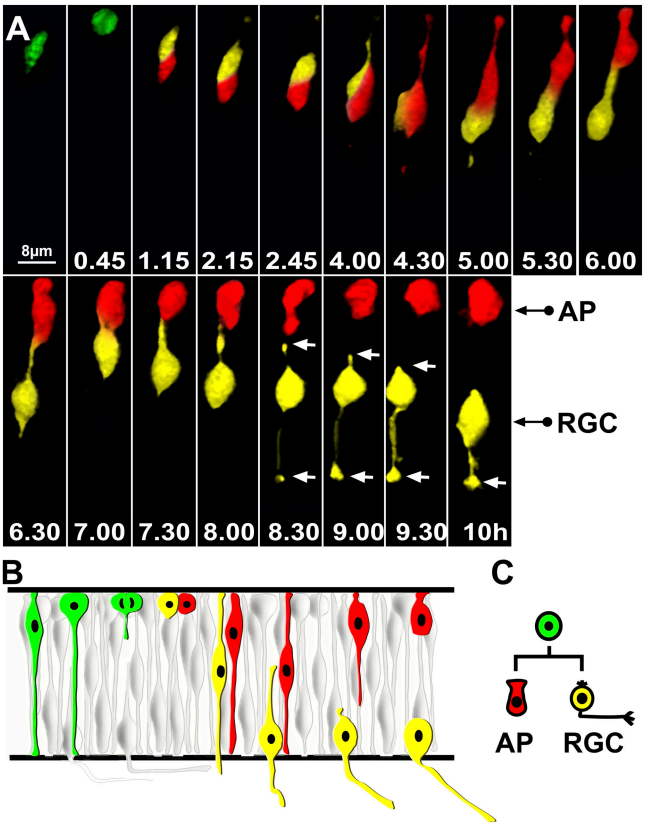

Figure 3. **ath5:GFP progenitors appear in G2 and divide once, generating one RGC and one non-RGC daughter cell.** (A) Time-lapse series showing the lineage of an ath5:GFP progenitor transplanted in a wild-type environment. Imaging was started 30–32 h after fertilization, and t = 0 corresponds to the time of appearance of ath5:GFP (4 h after the onset of the video recording). Daughter cells have been highlighted with different colors (red or yellow). The apical surface is up, whereas the basal surface is down. After division (t = 45 min), both daughter cells migrate toward the basal surface. At t = 5 h, one daughter cell (red) migrates toward the apical surface, whereas the other one (yellow) retracts the apical process and starts to grow an axon toward the basal surface. The white arrows point at the retracting apical process and the growth cone at the tip of the axon. Every single image is a 3D reconstruction of confocal stacks. AP, apical cell; RGC, retinal ganglion cell. (B) Diagram similar to the one shown in Fig. 1 B illustrating this division lineage, which is schematically represented in C.

host embryos. This early stage transplantation ensured that the transgenic cells had fully integrated normally into their wild-type hosts while allowing the density of transgenic cells in the retinas to be low enough for good observation. We then imaged several individual ath5:GFP-expressing progenitors in host retinas starting from 32–35 h after fertilization. We saw no cell deaths in the population of ath5:GFP-positive cells or their progeny within the time period studied (unpublished data). Anaphase and cytokinesis of ath5:GFP progenitors always occurred at the apical surface of the retina and parallel to it, as previously observed for all cell divisions in the zebrafish retina (Das et al., 2003). We were able to trace the GFP label in the daughters of 14 ath5:GFP dividing progenitors for many hours. All ath5:GFP-positive progenitors gave rise to two daughter cells. After separation, the two daughter cells reextended toward the basal surface but then usually migrated in opposite directions and acquired different morphologies. One daughter invariably migrated basally, withdrew its apical process, and began acquiring, through laminar position and axon extension, the characteristics of an RGC. The other daughter withdrew its basal process and migrated back to the apical surface. Fig. 3 shows an example of this lineage pattern (Video 4, available at http://www.jcb.org/cgi/content/full/jcb.200509098/DC1). This apical cell often changed in shape and began to look like an immature photoreceptor. When we tried to track the fate of this cell by extending our video recording, we observed the GFP signal becoming fainter, eventually disappearing from the focal plane. Although we were not able to show a clear fate for the apical daughter cell, our observations indicated that these apical cells did not divide again even within the extended time frame of these recordings, which is consistent with the observations that ath5-positive cells were always BrdU negative (Masai et al., 2005). Thus, the lineage pattern of these ath5:GFP progenitors seems to be reproducibly programmed to give rise to two postmitotic daughters, one of which becomes an RGC.

Removal of RGCs affects the fate and lineage of ath5:GFP progenitors

Previous in vitro studies suggested that inhibitory feedback signals secreted from differentiated RGCs prevent undifferentiated retinal cells from choosing the RGC fate (Waid and McLoon, 1998; Gonzalez-Hoyuela et al., 2001). If ath5:GFP-positive retinal progenitors respond to such cues, we might expect that the absence of RGCs should change the developmental potential and lineage of these progenitors. We used the *lakritz* mutant to investigate this question. In *lakritz,* RGCs fail to differentiate because of a loss of function mutation in the *ath5* locus. As a result, the first wave of cells exiting the cell cycle and differentiating as RGCs is missing in *lakritz*. Instead, the cells that would have differentiated as RGCs appear to stay in the cell cycle for an extra round of division and differentiate into other retinal cell types (Kay et al., 2001). Wondering whether the absence of the inhibitory feedback signals from previously generated RGCs would influence the lineage of wild-type ath5-expressing progenitors, we transplanted blastula-stage cells from ath5:GFP transgenic fish into the blastulas of *lakritz* mutant host embryos. Fig. 4 shows that there were proportionally more RGCs generated by ath5:GFP cells transplanted to *lakritz* hosts (~70%) than there were RGCs generated by the same progenitors transplanted to wild-type embryos (~40%). The proportion of other ath5:GFP-positive cell types was concomitantly lower (Fig. 4 and see Fig. 6). These data suggest that the lack of RGCs in *lakritz* hosts indeed biases the developmental behavior of the *ath5*-expressing progenitors toward an RGC fate.

A likely explanation for the increase in the proportion of ath:GFP-positive RGCs in *lakritz* versus wild-type hosts is that the lineage of the ath5:GFP progenitors is changed in these circumstances. Therefore, we traced the lineages of a number of dividing ath5:GFP cells in *lakritz* hosts. Again, no cell deaths were observed in the transplanted population of ath5:GFP-positive cells, and progenitors displayed normal interkinetic nuclear movements. Strikingly, these dividing progenitors

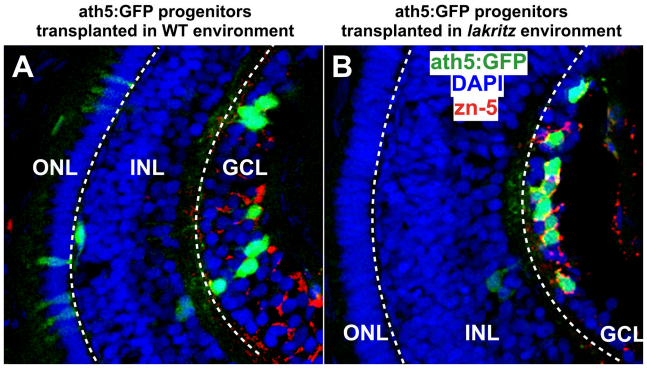

Figure 4. **More RGCs are generated at the expense of other retinal cell types by ath5:GFP progenitors in the *lakritz* mutant environment.** Increased number of RGCs generated by ath5:GFP progenitors when transplanted in the *lakritz* environment. (A and B) Longitudinal sections trough the central retina (at 4 d after fertilization) showing ath5:GFP retinal cells (green) in a wild-type environment (A) or in a *lakritz* mutant environment (B). RGCs are zn-5+ (red), and nuclei have been stained with DAPI to highlight the retinal cell layers. ath5:GFP retinal cells are found mainly in the GCL in a *lakritz* environment (B), whereas they are distributed in all three layers in the wild-type environment (A). GCL, ganglion cell layer; INL, inner nuclear layer; ONL, outer nuclear layer. White dashed lines separate the three retinal layers.

showed different lineage patterns in *lakritz* than in wild-type hosts. In many instances, both daughter cells began to differentiate as RGCs (Fig. 5 A and Video 5, available at http://www.jcb.org/cgi/content/full/jcb.200509098/DC1), and, in two cases, a progenitor divided twice, giving rise to one RGC with each division (Fig. 5 B and Video 6). A diagram comparison of the 14 lineages that we were able to follow in each of the two environments are shown in Fig. 6 A. Clearly, there is a striking difference between these two populations. Moreover, if it is the case that all RGCs normally arise from ath5-expressing progenitors, the changes in lineage programs represented in this study are enough to account for the increase in RGCs when ath5:GFP progenitors are transplanted into an environment lacking RGCs (Fig. 6 B).

Orientation of cell division

Apical-basal cell divisions, occurring with the cleavage plane parallel to the retinal surface, have been suggested to be a source of asymmetric cell fates in the vertebrate nervous system (Chenn and McConnell, 1995; Zhong et al., 1996, 1997; Wakamatsu et al., 1999; Cayouette et al., 2001; Cayouette and Raff, 2003). It was previously reported that progenitors in the zebrafish retina do not divide along the apical-basal axis even when they are giving rise to postmitotic daughters (Das et al., 2003). In agreement with this study, we found that all divisions of ath5:GFP cells occurred parallel to the retinal surface (i.e., with the cleavage plane perpendicular to the retinal surface). Interestingly, the same study showed that the proportion of cells dividing in the circumferential axis (>45°) increased over time at the expense of divisions orientated in the central-peripheral or radial axis (<45°; Fig. 7 A and Videos 7 and 8, available at http://www.jcb.org/cgi/content/full/jcb.200509098/DC1). Das et al. (2003) also suggested that the more circumferentially orientated divisions could

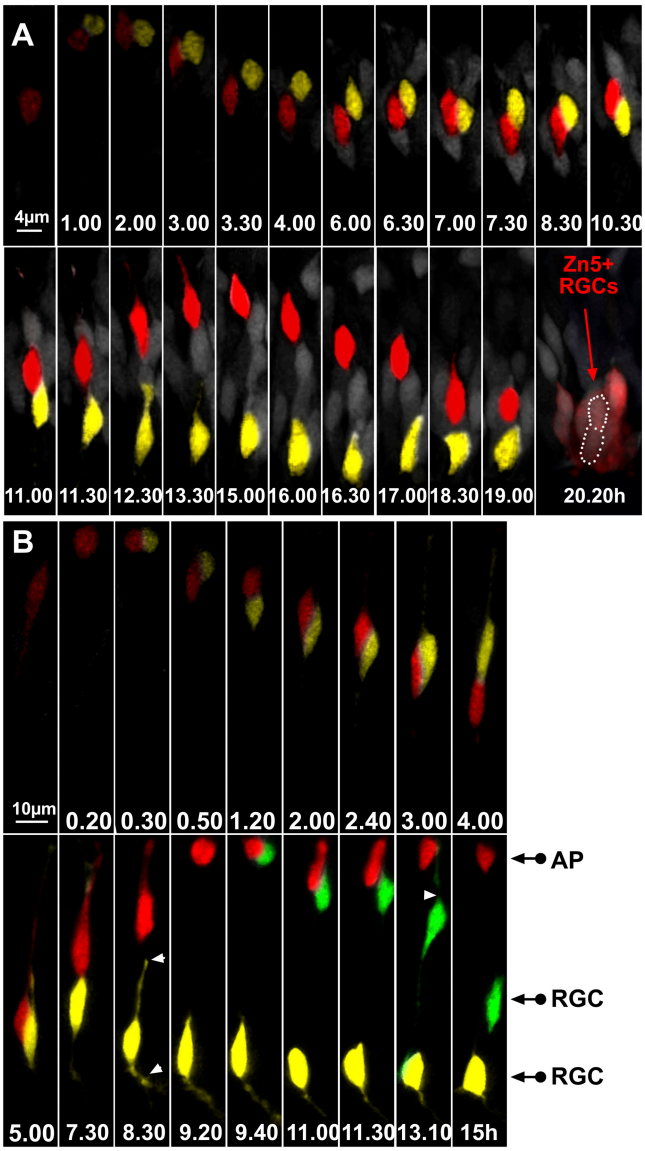

Figure 5. **ath5:GFP progenitors generate two RGCs after division in the *lakritz* environment.** (A) The two daughter cells have been highlighted in yellow or red. Time-lapse series showing an example of an ath5:GFP progenitor generating two RGCs in the *lakritz* environment. Imaging was started at 30–32 h after fertilization, and t = 0 corresponds to the time of appearance of ath5:GFP (4 h after the onset of the video recording). After 11 h, the red daughter cell starts migrating toward the apical surface. Once it has reached the apical surface (t = 15 h), it migrates back again toward the basal surface, where it differentiates in RGCs. The location of both daughter cells after 20 h is outlined by a white dotted line. Both cells were zn-5 positive after immunolabeling of the imaged retina. (B) An example of a time-lapse series showing an ath5:GFP progenitor that divides and generates another dividing progenitor. Imaging was started 30–32 h after fertilization, and t = 0 corresponds to the time of appearance of ath5:GFP (3 h after the onset of the video recording). At t = 9.40 h, the progenitor highlighted in red divides once more at the apical surface, generating one daughter cell (green) that lost its apical process and began to put out an axon and another daughter cell (red) that remained apical. White arrowheads point to the retracting apical process and the forming axon. AP, apical cell; RGC, retinal ganglion cell.

be asymmetric in nature, whereas the radial divisions could be more symmetric, and showed that the normal shift in orientation was compromised in *lakritz* mutants. In this study, we show that

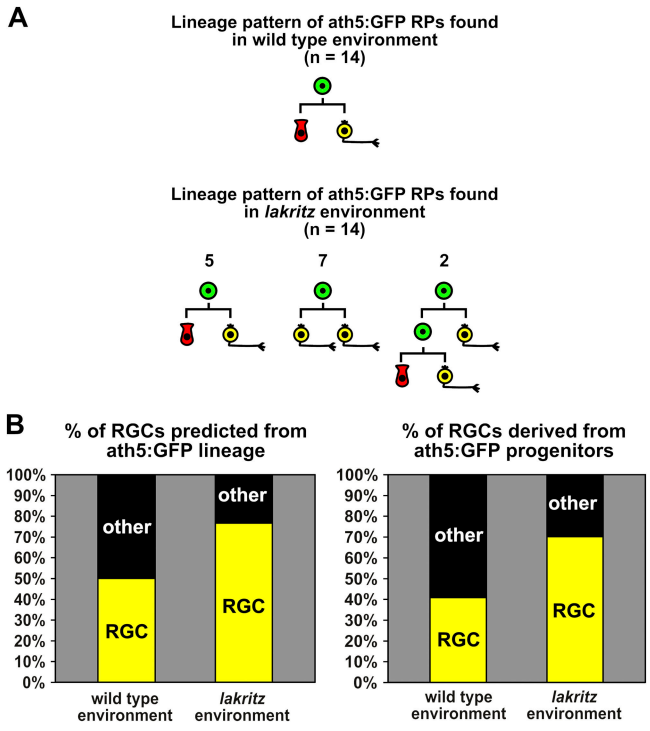

Figure 6. **Comparisons of lineage in a wild-type and *lakritz* environment.** (A) Summary of the lineage patterns of ath5:GFP progenitors observed in the wild-type and *lakritz* environment. Progenitors have been highlighted in green and RGCs in yellow. The apical cell has been highlighted in red. The fate of the apical cell can be one of a number of cell types, but our data seem to suggest that it is a photoreceptor more often than not. RP, retinal progenitor. From left to right: $n = 5$, 7, and 2. (B) Using these samples as indicators, one can calculate that in the wild-type environment, ~50% of the cells generated from ath5:GFP-positive progenitors would be predicted to become RGCs, whereas in the mutant environment, 77% would become RGCs. These differences are compared with the actual percent changes in the production of RGCs from ath5:GFP progenitors transplanted to the wild-type and *lakritz* environments (see Fig. 4). These are significantly different at the $P < 0.005$ level determined by the Chi-squared test. For wild-type hosts, $n = 795$ in nine retinas. For *lakritz* hosts, $n = 1{,}477$ in 11 retinas.

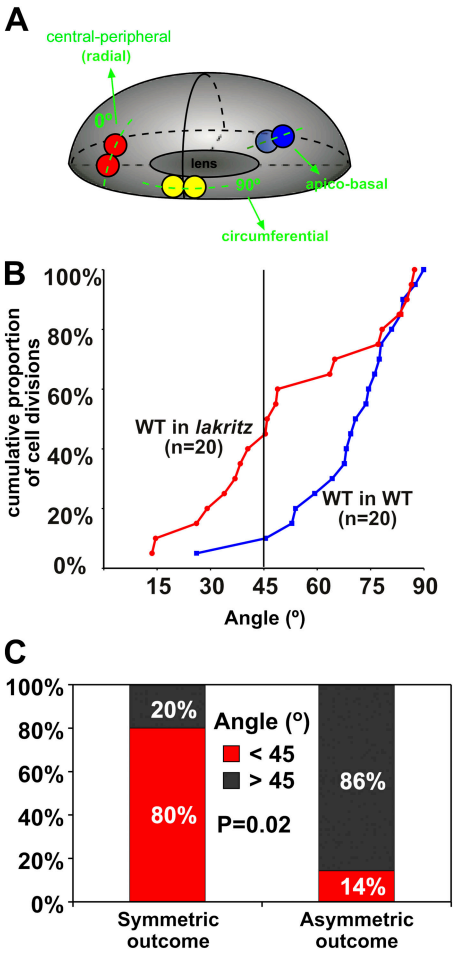

Figure 7. **Analysis of the orientation of cell division in ath5:GFP progenitors cells.** (A) 3D representation of the zebrafish retina as an ellipsoid body (Das et al., 2003). Only divisions where the mitotic spindle is oriented perpendicular to the retinal surface (indicated in yellow and red) can be seen in the zebrafish retina. An example of apico-basal division, which is not found in the zebrafish retina, is also indicated. An orientation of 0° represents a cell division along the central-peripheral (radial) axis, whereas an orientation of 90° represents a division along the circumferential axis (Videos 7 and 8, available at http://www.jcb.org/cgi/content/full/jcb.200509098/DC1). (B) Cumulative distributions of the orientation of cell divisions found in wild-type progenitors when transplanted either into a wild-type host (blue plot) or into *lakritz* hosts (red plot). The y axis indicates the proportion of cell divisions, whereas the x axis indicates the corresponding angles ($n = 20$ for both wild-type and *lakritz* hosts). Divisions that tend to be central-peripheral (<45°) are increased in ath5:GFP progenitors in the *lakritz* environment. The two distributions differ significantly, as determined by the Kolmogorov-Smirnov test ($P = 0.013$). (C) Divisions with symmetric outcomes tend to be oriented <45° (radial), whereas divisions with asymmetric outcomes preferentially occur with an angle >45° (circumferential). $P = 0.02$ by the Chi-squared test; $n = 5$ in symmetric cases; $n = 7$ in asymmetric cases.

only 10% of ath5:GFP progenitors transplanted into a wild-type environment divided radially (Fig. 7 B), whereas 45% of these same progenitors transplanted to the *lakritz* environment divided radially (Fig. 7 B). What is more telling is that we are able, for the first time, to classify asymmetric fate divisions and symmetric fate divisions among normal ath5:GFP-positive progenitors and, thus, to correlate the orientation of division directly with lineage outcome. In asymmetric divisions, one daughter cell became a RGC, whereas the other did not. In symmetric divisions, both daughter cells became RGCs. We found that circumferential divisions tended to give rise to asymmetric or different fates, whereas the radial divisions tended to give rise to symmetric or similar fates (Fig. 7 C).

Discussion

Recent studies provide evidence for the sufficiency of intrinsic programs for retinal cell diversification (Cayouette et al., 2003; Kay et al., 2005; Mu et al., 2005). This is consistent with the findings that wild-type retinal progenitors can turn on *ath5* and differentiate into RGCs when transplanted into a *lakritz* environment, suggesting that they do not need positive signals deriving from differentiated RGCs (Kay et al., 2005). It is particularly striking that all 14 ath5:GFP progenitors we followed in the wild-type environment displayed very similar lineages, strongly suggesting the presence of stereotyped and intrinsically determined lineage programs in the retina. However, such

a conclusion must be treated with caution, as we were examining these lineages only during a narrow time window, and the results of transplanting the same cells into a *lakritz* mutant suggest that even in a wild-type environment, earlier ath5-positive progenitors developing in an environment devoid of previously generated RGCs might show a different lineage program.

The reproducible lineage patterns that we found among *ath5*-expressing progenitors helps explain why *ath5* is necessary for RGC fate but does not necessarily correlate with RGC fate (Kanekar et al., 1997; Brown et al., 2001; Kay et al., 2001; Wang et al., 2001; Yang et al., 2003; Masai et al., 2005). All *ath5* progenitors produce RGCs, but not all *ath5*-expressing progenitors become RGCs. In wild-type animals, we found that an ath5:GFP-positive progenitor divides once and only one of the two daughters (the one that expresses ath5:GFP more strongly) becomes a RGC. The other daughter usually becomes a different cell type and down-regulates ath5:GFP expression. Interestingly, we observed that this cell usually ended up in the ONL and assumed an immature photoreceptor-like morphology, suggesting that, at least during the period of our video recordings, ath5:GFP progenitors tend to be restricted to a lineage that produce one RGC and one other cell type, usually a photoreceptor.

ath5 is first expressed in post–S-phase retinal precursors (Yang et al., 2003; Ma et al., 2004; Masai et al., 2005). In our study, we recorded many ath5:GFP retinal progenitors undergoing cytokinesis at the apical surface and found that *ath5* mRNA colocalizes with ath5:GFP expression in M-phase progenitors. Interestingly, we found that the onset of ath5:GFP expression in dividing progenitors was almost always shortly before they entered M phase and while their nuclei were undergoing interkinetic migration toward the apical surface, suggesting that *ath5* usually turns on in retinal progenitors at G2 of the final cell cycle (Miale and Sidman, 1961). Other cases have been described in which intrinsic factors begin to be expressed in G2; for example, Prox1, a homeobox protein that is required for the determination of horizontal cells in the vertebrate retina, is initiated at G2 (Dyer et al., 2003), but in these cases, the fates of the daughter cells have not been followed.

It has been previously argued that the distinct clones seen in the retina could have been sculpted out of a highly conserved lineage program by random cell death (Voyvodic et al., 1995). The differences we see among ath5:GFP progenitor clones in which one of the daughter cells becomes an RGC and the other becomes a different cell type or, in the *lakritz* environment, becomes another RGC are clearly not results of cell death but are caused by different lineage patterns.

Our results clearly also show that the lineage programs of ath5:GFP-expressing cells respond to negative feedback signals in the normal environment, at least during the developmental time window of this study when the first RGCs are already present. Previous studies have shown that the environment plays an important role in regulating the proportion of RGCs generated (Waid and McLoon, 1998; Gonzalez-Hoyuela et al., 2001). Indeed, we found that after transplantation of wild-type cells into a wild-type host, about half of ath5:GFP-positive cells are RGCs, but this percentage is increased by ~30% when the same cells are transplanted to a *lakritz* mutant environment. By following individual ath5:GFP progenitors over time, we found that the environment can dramatically influence their lineage patterns, leading to a predicted increase in RGC production of ~30%. A greater number of dividing ath5:GFP progenitors give rise to two RGCs compared with one in the wild-type environment.

Recent data has shown that GDF11 is a potential negative feedback factor for RGC production (Kim et al., 2005). In mice mutant for GDF11, the histogenetic window for *ath5* expression and RGC production is extended. In these mutants, extra RGCs are generated at the expense of later born cell types. Follistatin antagonizes GDF11, and follistatin mutants show a shortened period of *ath5* expression and RGC production in the retina. These results fit well with our findings of extra rounds of division and a switch from asymmetrical fate to symmetrical RGC-generating divisions in ath5 progenitors transplanted to the *lakritz* environment.

Apical-basal cell divisions have been found in the vertebrate nervous system, including the retina, and some of them have been shown to be asymmetric in nature (Chenn and McConnell, 1995; Zhong et al., 1996, 1997; Wakamatsu et al., 1999; Cayouette et al., 2001; Cayouette and Raff, 2003). Planar divisions, however, can also be asymmetric (Adams, 1996; Gho and Schweisguth, 1998; Wodarz and Huttner, 2003; Kosodo et al., 2004; Malicki, 2004; Sun et al., 2005). In the chick retina, cells dividing apico-basally are a small percentage of dividing cells, and this percentage does not seem to account for all of the asymmetric behavior of daughter cells (Silva et al., 2002). Both in the zebrafish retina and neural tube, apical-basal divisions are entirely absent (Das et al., 2003; Geldmacher-Voss et al., 2003; Lyons et al., 2003). Within the plane of the ventricular surface in the zebrafish retina, however, cells may divide along a more circumferential or radial axis (Das et al., 2003). Interestingly, we found that circumferential divisions in ath5:GFP-positive progenitors tend to give rise to different or asymmetric fates. One possible explanation for this relates to the neurogenic wave, which spreads primarily in the circumferential axis (Neumann and Nuesslein-Volhard, 2000). Consequently, circumferential divisions could produce two daughter cells that are differentially exposed to any potential signals that are associated with this wave. Differences in the intrinsic ability to respond to extrinsic signals may also account for asymmetric behavior of daughter cells. Indeed, a recent study found that unequal segregation of the EGF receptor during mitosis in dividing cortical progenitor cells plays a part in generating asymmetric behavior of the daughter cells (Sun et al., 2005). Alternatively, these circumferential divisions may favor the unequal partitioning of an intrinsic determinant. It will be interesting to investigate which of these possibilities is at play in this system.

In this study, we found that radial divisions tend to give rise to similar or symmetric fates (in this case, two RGCs). In the Das et al. (2003) study (Lyons et al., 2003), all dividing cells were examined, including those early dividing cells in which presumably both daughters remained in the cell cycle. The conclusion from that study was that early progenitors

might also divide primarily in a radial orientation. If that is so, the results here suggest that radial cell divisions can give rise to two progenitors at early stages or two similar postmitotic daughters at later stages.

It has always been an aspiration of scientists in this field to directly observe clone formation and to watch how different cell types arise in vivo. This time-lapse analysis is the beginning of such work, and we have used this beginning to show, for the first time, a major role for the environment in influencing the orientation of division and lineage pattern of a distinct class of retinal precursors in their final mitosis.

Materials and methods

Fish

Fish were maintained at 26.5°C. Embryos were raised at 28.5°C and staged in hours after fertilization. Embryos used for imaging were of wild-type strains (*wik*), were homozygous for the *lakritz (lakth241)* mutation (a gift from H. Baier, University of California, San Francisco, San Francisco, CA), or were ath5:GFP transgenic (Masai et al., 2003). All embryos were treated with 0.003% phenylthiourea (Sigma-Aldrich) from 11 to 24 h after fertilization to delay pigment formation in the eye.

Plasmids

A pCS2 + GAP-mRFP plasmid, which consists of mRFP preceded by a palmitoylation signal from GAP43, was used to label the membrane of retinal progenitors in ath5:GFP transgenic donor embryos before they started to express ath5:GFP. The DNA was injected at a concentration of 10 ng/μl in the cell of one-cell stage embryos.

In vivo imaging

Both transgenic and transplanted embryos were screened 24 h after fertilization under a fluorescent dissecting stereo microscope (MZ FLIII; Leica) for those with strong eGFP expression in the retina. Chosen embryos were mounted in 0.7% agarose, pH 7.4, containing 0.04% MS-222 and 0.01 M Hepes onto a No. 0 coverslip that served as the bottom of a 30-mm petri dish. Embryos were also orientated such that the lateral side of the eye was closest to the coverslip. The petri dish was then filled with embryo medium containing 0.04% MS-222 and placed in a heated stage at 30°C on an inverted microscope (DMIRBE; Leica). Both mRFP and eGFP fluorescence in the specimens was imaged with a confocal laser scanning microscope (model TCS-NT; Leica) using a 63× NA 1.2 water immersion objective (Leica) with a long working distance (0.225 mm). A 488-nm line from an argon laser was used for GFP excitation, and a krypton laser providing a 568-nm laser line was used for RFP excitation. Emission was detected using individual descanned photomultiplier tube detectors. For time lapses, optical sections 0.5 μm apart were taken through a volume of the retina up to 50 μm in depth and Kallmann averaged once. Time points were between 10 and 15 min apart. Image data was acquired and stored as TIFF files using TCS-NT or confocal software (Leica).

Visualization and cell tracking

Acquisition was performed using macros provided by R. Adams (University of Cambridge, Cambridge, UK). To visualize the acquired data as time-resolved volumes, images were processed on a Macintosh computer using Volocity (Improvision). All projections in each dataset were assembled into Quicktime videos. Cell tracking was performed using the Volocity classification module (Improvision) as well as a tracking program provided by R. Adams. At the end of each video recording, a whole mount antibody staining with the ganglion cell marker zn-5 was performed on the imaged retina in order to further verify the identity of the final fate of the tracked cells.

Imaging of wild-type and *lakritz* transplanted embryos

The *lakritz* phenotype does not become apparent until 4 d after fertilization, but it can be easily identified by tissue genotyping (Kay et al., 2001). To identify the genotype of embryos obtained from *lakritz* heterozygous matings 24 h after fertilization, a small portion of the tip of the tail was cut and used for tissue genotyping. The protocol used was described previously (Kay et al., 2001), with few modifications. This method allowed us to efficiently genotype the embryo in a short time and start the time-lapse imaging ~32 h after fertilization.

Transplantation

Transplantations were performed as previously described (Ho and Kane, 1990). Approximately 10–50 cells were transplanted from blastula-stage ath5:GFP transgenic embryos into the animal pole of blastula-stage embryos that were obtained from *lakritz* heterozygous matings. For imaging on retinal sections, host embryos were left to grow in embryo medium until 4 d after fertilization, when they were fixed, cryosectioned, labeled with antibody, and analyzed by confocal microscopy. For whole-mount immunostaining and live imaging, embryos where grown in embryo medium containing 0.003% phenylthiourea (Sigma-Aldrich) from 11 to 24 h after fertilization and either fixed at 4 d or genotyped as described above for time-lapse imaging.

Histochemical methods

Whole-mount in situ hybridization was performed on ath5:GFP transgenic embryos using *ath5* as a probe. A fluorescent signal was obtained by using Fast Red as a substrate for alkaline phosphatase (Sigma-Aldrich) followed by antibody labeling for GFP and confocal analysis. Antibody labeling was performed on 10-μm–thick cryosections or on whole embryos and was analyzed with a confocal microscope (model TCS-SP-MP; Leica). The following antibodies were used: anti–rabbit GFP (Invitrogen), anti–rabbit polyclonal calretinin (1:500; Chemicon), anti–rabbit PKCβ1 (1:50; Santa Cruz Biotechnology, Inc.), anti–mouse zn-5 (1:200; University of Oregon), and anti–mouse Zpr-1 (1:500; University of Oregon). Bound antibodies were detected using anti–rabbit AlexaFluor488, anti–rabbit AlexaFluor594 (both at 1:1,000; Invitrogen), and anti–mouse Cy3 (Chemicon). Nuclei were stained at 1:50 DAPI in PBS for 10 min.

Analysis of the orientation of cell division

Analysis of the orientation of cell division was performed as previously described (Das et al., 2003).

Online supplemental material

Video 1 shows ath5:GFP progenitors dividing at the apical surface. Video 2 shows ath5:GFP expression occurring during apically oriented interkinetic nuclear migration. Video 3 shows ath5:GFP retinal progenitors extending axons toward the basal surface while differentiating in RGCs. Video 4 depicts the common lineage program of ath5:GFP progenitors in a wild-type environment. Video 5 shows the lineage program of an ath5:GFP progenitor generating two RGCs in a *lakritz* environment. Video 6 shows the lineage program of an ath5:GFP progenitor generating one RGC and another progenitor in the *lakritz* environment. Video 7 depicts a circumferential division. Video 8 shows a radial or central-peripheral division. Online supplemental material is available at http://www.jcb.org/cgi/content/full/jcb.200509098/DC1.

We thank Jeremy Skepper for help in using the confocal microscope and Ingrid Pradel for helping with embryo genotyping. Many thanks go to Richard Adams for providing macros for acquisition and cell tracking. We thank the Zebrafish International Resource Center for providing antibodies

This work was supported by a grant (#RR12546) from the National Institutes of Health National Center for Research Resources. We also thank the European Commission and the Wellcome Trust for funding this work.

The authors have no conflicting financial interests.

Submitted: 16 September 2005
Accepted: 14 November 2005

References

Adams, R.J. 1996. Metaphase spindles rotate in the neuroepithelium of rat cerebral cortex. *J. Neurosci.* 16:7610–7618.

Brown, N.L., S. Patel, J. Brzezinski, and T. Glaser. 2001. Math5 is required for retinal ganglion cell and optic nerve formation. *Development.* 128:2497–2508.

Cayouette, M., and M. Raff. 2003. The orientation of cell division influences cell-fate choice in the developing mammalian retina. *Development.* 130:2329–2339.

Cayouette, M., A.V. Whitmore, G. Jeffery, and M. Raff. 2001. Asymmetric segregation of Numb in retinal development and the influence of the pigmented epithelium. *J. Neurosci.* 21:5643–5651.

Cayouette, M., B.A. Barres, and M. Raff. 2003. Importance of intrinsic mechanisms in cell fate decisions in the developing rat retina. *Neuron.* 40:897–904.

Chenn, A., and S.K. McConnell. 1995. Cleavage orientation and the asymmetric inheritance of Notch1 immunoreactivity in mammalian neurogenesis.

Cell. 82:631–641.

Das, T., B. Payer, M. Cayouette, and W.A. Harris. 2003. In vivo time-lapse imaging of cell divisions during neurogenesis in the developing zebrafish retina. *Neuron.* 37:597–609.

Dyer, M.A., F.J. Livesey, C.L. Cepko, and G. Oliver. 2003. Prox1 function controls progenitor cell proliferation and horizontal cell genesis in the mammalian retina. *Nat. Genet.* 34:53–58.

Geldmacher-Voss, B., A.M. Reugels, S. Pauls, and J.A. Campos-Ortega. 2003. A 90-degree rotation of the mitotic spindle changes the orientation of mitoses of zebrafish neuroepithelial cells. *Development.* 130:3767–3780.

Gho, M., and F. Schweisguth. 1998. Frizzled signalling controls orientation of asymmetric sense organ precursor cell divisions in *Drosophila*. *Nature.* 393:178–181.

Gonzalez-Hoyuela, M., J.A. Barbas, and A. Rodriguez-Tebar. 2001. The autoregulation of retinal ganglion cell number. *Development.* 128:117–124.

Ho, R.K., and D.A. Kane. 1990. Cell-autonomous action of zebrafish spt-1 mutation in specific mesodermal precursors. *Nature.* 348:728–730.

Hutcheson, D.A., M.I. Hanson, K.B. Moore, T.T. Le, N.L. Brown, and M.L. Vetter. 2005. bHLH-dependent and -independent modes of Ath5 gene regulation during retinal development. *Development.* 132:829–839.

Kanekar, S., M. Perron, R. Dorsky, W.A. Harris, L.Y. Jan, Y.N. Jan, and M.L. Vetter. 1997. Xath5 participates in a network of bHLH genes in the developing *Xenopus* retina. *Neuron.* 19:981–994.

Kay, J.N., K.C. Finger-Baier, T. Roeser, W. Staub, and H. Baier. 2001. Retinal ganglion cell genesis requires lakritz, a Zebrafish atonal homolog. *Neuron.* 30:725–736.

Kay, J.N., B.A. Link, and H. Baier. 2005. Staggered cell-intrinsic timing of ath5 expression underlies the wave of ganglion cell neurogenesis in the zebrafish retina. *Development*. 132:2573–2585.

Kim, J., H.H. Wu, A.D. Lander, K.M. Lyons, M.M. Matzuk, and A.L. Calof. 2005. GDF11 controls the timing of progenitor cell competence in developing retina. *Science.* 308:1927–1930.

Kosodo, Y., K. Roper, W. Haubensak, A.M. Marzesco, D. Corbeil, and W.B. Huttner. 2004. Asymmetric distribution of the apical plasma membrane during neurogenic divisions of mammalian neuroepithelial cells. *EMBO J.* 23:2314–2324.

Lyons, D.A., A.T. Guy, and J.D. Clarke. 2003. Monitoring neural progenitor fate through multiple rounds of division in an intact vertebrate brain. *Development.* 130:3427–3436.

Ma, W., R.T. Yan, W. Xie, and S.Z. Wang. 2004. A role of ath5 in inducing neuroD and the photoreceptor pathway. *J. Neurosci.* 24:7150–7158.

Malicki, J. 2004. Cell fate decisions and patterning in the vertebrate retina: the importance of timing, asymmetry, polarity and waves. *Curr. Opin. Neurobiol.* 14:15–21.

Masai, I., Z. Lele, M. Yamaguchi, A. Komori, A. Nakata, Y. Nishiwaki, H. Wada, H. Tanaka, Y. Nojima, M. Hammerschmidt, et al. 2003. N-cadherin mediates retinal lamination, maintenance of forebrain compartments and patterning of retinal neurites. *Development.* 130:2479–2494.

Masai, I., M. Yamaguchi, N. Tonou-Fujimori, A. Komori, and H. Okamoto. 2005. The hedgehog-PKA pathway regulates two distinct steps of the differentiation of retinal ganglion cells: the cell-cycle exit of retinoblasts and their neuronal maturation. *Development.* 132:1539–1553.

Miale, I.L., and R.L. Sidman. 1961. An autoradiographic analysis of histogenesis in the mouse cerebellum. *Exp. Neurol.* 4:277–296.

Moore, K.B., M.L. Schneider, and M.L. Vetter. 2002. Posttranslational mechanisms control the timing of bHLH function and regulate retinal cell fate. *Neuron.* 34:183–195.

Mu, X., X. Fu, H. Sun, S. Liang, H. Maeda, L.J. Frishman, and W.H. Klein. 2005. Ganglion cells are required for normal progenitor-cell proliferation but not cell-fate determination or patterning in the developing mouse retina. *Curr. Biol.* 15:525–530.

Neumann, C.J., and C. Nuesslein-Volhard. 2000. Patterning of the zebrafish retina by a wave of sonic hedgehog activity. *Science.* 289:2137–2139.

Ohnuma, S., S. Hopper, K.C. Wang, A. Philpott, and W.A. Harris. 2002. Coordinating retinal histogenesis: early cell cycle exit enhances early cell fate determination in the *Xenopus* retina. *Development.* 129:2435–2446.

Seymour, R.M., and M. Berry. 1975. Scanning and transmission electron microscope studies of interkinetic nuclear migration in the cerebral vesicles of the rat. *J. Comp. Neurol.* 160:105–125.

Silva, A.O., C.E. Ercole, and S.C. McLoon. 2002. Plane of cell cleavage and numb distribution during cell division relative to cell differentiation in the developing retina. *J. Neurosci.* 22:7518–7525.

Sun, Y., S.K. Goderie, and S. Temple. 2005. Asymmetric distribution of EGFR receptor during mitosis generates diverse CNS progenitor cells. *Neuron.* 45:873–886.

Voyvodic, J.T., J.F. Burne, and M.C. Raff. 1995. Quantification of normal cell death in the rat retina: implications for clone composition in cell lineage analysis. *Eur. J. Neurosci.* 7:2469–2478.

Waid, D.K., and S.C. McLoon. 1998. Ganglion cells influence the fate of dividing retinal cells in culture. *Development.* 125:1059–1066.

Wakamatsu, Y., T.M. Maynard, S.U. Jones, and J.A. Weston. 1999. NUMB localizes in the basal cortex of mitotic avian neuroepithelial cells and modulates neuronal differentiation by binding to NOTCH-1. *Neuron.* 23:71–81.

Wang, S.W., B.S. Kim, K. Ding, H. Wang, D. Sun, R.L. Johnson, W.H. Klein, and L. Gan. 2001. Requirement for math5 in the development of retinal ganglion cells. *Genes Dev.* 15:24–29.

Wodarz, A., and W.B. Huttner. 2003. Asymmetric cell division during neurogenesis in *Drosophila* and vertebrates. *Mech. Dev.* 120:1297–1309.

Yang, Z., K. Ding, L. Pan, M. Deng, and L. Gan. 2003. Math5 determines the competence state of retinal ganglion cell progenitors. *Dev. Biol.* 264:240–254.

Zhong, W., J.N. Feder, M.M. Jiang, L.Y. Jan, and Y.N. Jan. 1996. Asymmetric localization of a mammalian numb homolog during mouse cortical neurogenesis. *Neuron.* 17:43–53.

Zhong, W., M.M. Jiang, G. Weinmaster, L.Y. Jan, and Y.N. Jan. 1997. Differential expression of mammalian Numb, Numblike and Notch1 suggests distinct roles during mouse cortical neurogenesis. *Development.* 124:1887–1897.